

A one-pot synthesis of a ternary nanocomposite based on mesoporous silica, polyaniline and silver†

Cite this: *RSC Adv.*, 2013, **3**, 26142

Ana Cláudia De Abreu Rosa,^a Cintia Marques Correa,^a Roselena Faez,^b Marcos Augusto Bizeto^a and Fernanda Ferraz Camilo^{*a}

The research on hybrid materials composed of inorganic and organic species in the nanometer range is motivated by the synergic combination of their native properties in a unique material. In this paper, we report a new one-pot synthesis of a ternary nanocomposite based on a conducting polymer (polyaniline – PANI) and silver, using mesoporous silica (MCM-41) as a hard template to promote the controlled growth of both polymer chains and silver nanoparticles. The presence of these reaction products was proved by the appearance of the characteristic diffraction peaks of face-centered cubic metallic silver phase in the X-ray diffractogram and by the presence of typical bands of polyaniline as emeraldine salt in the FTIR and UV-Vis spectra. The preservation of the ordered MCM-41 mesostructure after the polymerization reaction was also attested by XRD and TEM analysis and it was accompanied by a decreasing of the particle size as observed in the SEM images. N₂ adsorption–desorption isotherms support the statement that PANI chains and AgNP have been incorporated mainly into the channel of MCM-41, a fact also attested by TEM images. The electrical conductivity of this nanocomposite is on the order of 10⁻³ S cm⁻¹, which is one million times higher than the value obtained for a MCM-41/polyaniline composite. Although some reports about the isolated incorporation of polyaniline or silver nanoparticles into the MCM-41 pores are found in the literature, to our knowledge this is the first time that such nanocomposite preparation is reported.

Received 23rd August 2013
Accepted 22nd October 2013

DOI: 10.1039/c3ra44618b

www.rsc.org/advances

1. Introduction

Nanomaterial science is an interesting research area due to the distinct electronic, optical, magnetic and catalytic properties that materials might show when are in the nanometric domain. In particular, the investigation of hybrid materials composed of inorganic and organic species at the nanometer level is also important due to the potential synergetic combination of their properties in a unique material.^{1–3}

Among these hybrid materials, those comprised by conducting polymers as organic component have gained attention due to their potential application in electronic nanodevices and sensors.^{4,5} Porous inorganic matrixes with uniform pores dimensions at nanoscopic domain are considered good hosts for polymer formation. In the case of conducting polymers, the confined ambient of the pores affords the formation of chains with less branching, which is an important feature to guarantee

electrical conductivity improvement. In this sense, it is already published some studies focusing on the preparation of hybrid materials composed by inorganic hosts with pores in nanoscale, such as mesoporous silica (SBA-15 and MCM-41) with different conducting polymers (polyaniline, polypyrrole).^{6–8} Although, in these papers, the reported electrical conductivity of the nanocomposite is lower than the pure polymer, the further inorganic framework removal became an useful strategy to obtain conducting polymers nanowires, which have application as nano-electronics components.^{6,9} Studies involving hybrid materials containing polyaniline (PANI), one of the most studied conducting polymer, and MCM-41 have already been published^{6,10–17} and although these composites are insulators (electrical conductivity around 10⁻⁹ S cm⁻¹),¹⁴ they are still attractive materials due to their notable photocatalytic activity under visible light¹⁶ and to the electrorheological properties that they shown when dispersed in fluids.¹⁴ Additionally, the embedding of PANI with metallic nanoparticles can also be an attractive strategy to enhance some features of the bulk polymer.^{18–23} For example, PANI/Ag composites^{24–34} show improved electrical and thermal conductivities when compared to pure PANI with additional antibacterial activity and optical properties. In this field, several papers are focusing on the development of new synthetic methods or adjusting old ones to prepare homogenous nanocomposite of PANI/Ag from the direct

^aLaboratório de Materiais Híbridos, Instituto de Ciências Ambientais, Químicas e Farmacêuticas, Universidade Federal de São Paulo, Rua São Nicolau, 210, CEP: 09913-030, Diadema, SP, Brazil. E-mail: ffcamillo@unifesp.br; Tel: +55 11 3319-3568

^bLaboratório de Materiais Poliméricos e Biossorventes, Departamento de Ciências da Natureza, Matemática e Educação, Universidade Federal de São Carlos, São Carlos, SP, Brazil

† Electronic supplementary information (ESI) available. See DOI: 10.1039/c3ra44618b

oxidation of aniline by silver cations in one-step reaction.^{24–28} In 2012, our group showed an innovative method to produce a nanocomposite of polyaniline with metallic silver in a imidazolium-based liquid ionic, which was used as solvent and soft template. For this reaction occur, we needed to overcome the low solubility of regular silver salts, by using $\text{AgN}(\text{SO}_2\text{CF}_3)_2$ as silver cations source, which is a soluble salt in ionic liquid. Although the resulting material has been obtained with success, the silver nanoparticles dispersed in the polymer matrix were not monodisperse and the polymeric chains were allowed to growth without control.³⁵ It is worth to mention that pure ionic liquids, especially containing imidazolium cations, have an ordered structures, which have already been extensively reviewed in the literature.^{36,37} This supramolecular organization is due to the coulomb interactions between the ions and in the case of the imidazolium cations, the existence of an extended network of cations and anions connected together by “pseudo” hydrogen bonding and π - π stacking interactions. Because of this organization, ILs have been used as soft template for the synthesis of materials, such as silica,³⁸ metallic nanoparticles³⁹ and polymer.⁴⁰

In 2010, Park *et al.*⁴¹ reported the synthesis of nanosized silica/Ag/PANI hybrid prepared using γ -radiolysis and poly(vinylpyrrolidone) (PVP) as stabilizer, aiming its use as active material in a hydrogen peroxide biosensor.⁴² At the same year, Lee *et al.*⁴³ described the synthesis of silver nanoparticles distributed into PANI bridged silica network and its activity as catalyst for the reduction of 4-nitrophenol, which is a common water contaminant.

Although reports focusing on hybrid materials composed of conducting polymers or metallic particles incorporate in MCM-41 pores are found in the literature as above mentioned, those concerning the combination of these three species are still scarce.^{41–43} For our knowledge, there is no report in the literature concerning the preparation of PANI, mesoporous silica (MCM-41) and silver.

Based on these facts, we developed an innovative method to prepare a MCM-41/PANI/Ag nanocomposite by the direct oxidation of aniline with Ag^+ in an ionic liquid, called

1-butyl-3-methylimidazolium bis(trifluoromethanesulfonyl)-amide (BMImTf₂N) (Fig. 1). In this present paper, we tried a step further in promoting the controlled growth of both polyaniline chains and silver nanoparticles, using MCM-41 as a hard template, which has a defined structural arrangement with cylindrical pores with 30 Å. Our results indicate that $\text{AgN}(\text{SO}_2\text{CF}_3)_2$ salt dissolved in the BMImTf₂N ionic liquid is able to diffuse into the silica pores containing aniline monomer previously adsorbed and to promote the polymerization reaction without provoke the hard template structure collapse or reduction of structural ordering. The presence of metallic silver particles in MCM-41/PANI should increase the electrical conductivity of this isolating binary composite.

2. Experimental section

2.1. Materials

Aniline (Aldrich, 97%) was distilled twice under reduced pressure before use. BMImTf₂N was prepared according to procedure already described in the literature.⁴⁴ Other chemicals were used as received.

2.2. Preparation of MCM-41

MCM-41 was prepared following procedure described in the literature.⁴⁵ Succinctly, tetraethylortosilicate (TEOS, Aldrich) was hydrolyzed, under basic condition (NH_4OH , Aldrich), using micellar aggregates of cetyltrimethylammonium bromide (CTAB, Aldrich) as template. The reactants molar ratio were $525(\text{H}_2\text{O}) : 69(\text{NH}_4\text{OH}) : 0.125(\text{CTAB}) : 1(\text{TEOS})$. After 2 h, the mesophase was isolated by filtration and the solid was calcined under nitrogen atmosphere until the furnace temperature reaches 550 °C, remaining at this temperature for more 3 h under air atmosphere.

2.3. Preparation of $\text{AgN}(\text{SO}_2\text{CF}_3)_2$ (AgTf₂N)

Into a 50 mL vacuum sublimator it was added 5.14 g (18.0 mmol) of anhydrous $\text{LiN}(\text{SO}_2\text{CF}_3)_2$ (Aldrich, 97%) followed by 25 mL of H_2SO_4 (Aldrich, 98%). The solution was heated at 70 °C with stirring, and $\text{HN}(\text{SO}_2\text{CF}_3)_2$ was collected in the cooler part of the sublimator as a white solid (90% yield). In the next step, Ag_2CO_3 (12.0 mmol, newly synthesized) was added, under stirring, to a solution of $\text{HN}(\text{SO}_2\text{CF}_3)_2$ (5.62 g; 20.0 mmol) in 50 mL of distilled water under stirring. The reaction mixture was heated at 65 °C and then a white solid was isolated by removing water under reduced pressure. To remove impurities, such as silver oxide, the solid was dissolved in 50 mL of diethyl ether and the remained solid was collected by filtration. After solvent removal under reduced pressure, $\text{AgN}(\text{SO}_2\text{CF}_3)_2$ was obtained as white powder with 70% yield. The melting point determined for this compound was 249–250 °C, which is similar to the commercial product (CAS: 189114-61-2).

2.4. Aniline adsorption

The monomer adsorption into the silica was performed in a closed system containing two vials, one with liquid aniline and another one with MCM-41 (previously dehydrated in an oven at

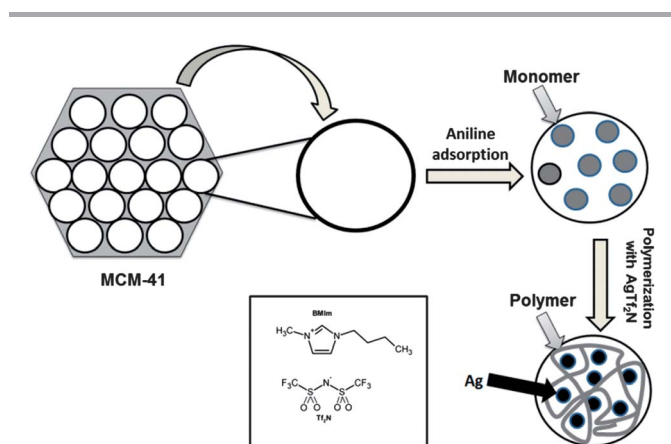


Fig. 1 Pictorial representation of the preparation of the MCM-41/PANI/Ag composite.

100 °C).¹⁷ The system was vacuumed and heated to 40 °C to saturate the internal atmosphere with aniline vapor and promote the adsorption into the mesoporous silica. Hereafter in the text, this material will be referred as MCM-41/Ani.

2.5. Preparation of MCM-41/PANI/Ag

260 mg of MCM-41/Ani (containing 80 mg of aniline; 0.86 mmol) was added to 665 mg of $\text{AgN}(\text{SO}_2\text{CF}_3)_2$ (1.72 mmol) dissolved in 1.7 mL of BMImTf_2N at room temperature and under stirring. In a few minutes, the reaction mixture turned green and after 24 h, the solid was isolated by filtration, rinsed with acetone and dried under reduced pressure. Hereafter in the text, this material will be referred as MCM-41/PANI/Ag.

The MCM-41/PANI/Ag composite (426 mg) was obtained as a green solid (yield = 48%, considering 9% of organic content determined by thermogravimetry analysis and the initial mass of the monomer).

2.6. Characterization techniques

MCM-41 was characterized by X-ray diffractometry (XRD), thermogravimetry analysis (TGA), scanning (SEM) and transmission (TEM) electron microscopy and by N_2 adsorption-desorption isotherm.

The ternary composite was characterized by XRD, TGA, infrared (FTIR) and ultraviolet-visible (UV-Vis) spectroscopies, SEM, TEM, N_2 adsorption-desorption isotherm and by the evaluation of the electrical conductivity using the four-probe method.

X-ray diffraction patterns (XRDP) of powdered samples were recorded on a Rigaku diffractometer model Miniflex using $\text{Cu-K}\alpha$ radiation.

Thermogravimetric analyses (TGA) was performed in a Shimadzu thermoanalyser TA-60, under synthetic air atmosphere with a flux of $100 \text{ cm}^3 \text{ min}^{-1}$ and a heating rate of $10 \text{ }^\circ\text{C min}^{-1}$.

Fourier transform infrared spectra (FTIR) were recorded on a Bomem spectrophotometer, model MB-102 using the DRIFT accessory. The samples were diluted in solid KBr before the spectrum recording.

UV-Visible electronic absorption spectra (UV-Vis) of solid samples were recorded in a Shimadzu spectrophotometer model UV-2401PC equipped with an integration sphere apparatus. The spectra were recorded on reflectance mode and transformed to absorbance using the equipment software (Kubelka-Munk method option). The samples were diluted in BaSO_4 , which is also used as the reference substance.

Transmission electron microscopy (TEM) images were recorded on a JEOL microscope model JEM 2100 operating at 200 kV coupled with a Thermo-Noran EDS. Samples were prepared by dispersing the solid in isopropanol with the aid of an ultrasonic bath followed by deposition onto a carbon-coated Cu microgrid.

Scanning electron microscopy (FEG-SEM) micrographs of uncoated samples were recorded on a JEOL field emission gun scanning electron microscope model JSM-7600F, using secondary electrons detection mode.

Nitrogen adsorption-desorption was measured at 77 K using nitrogen of 99.998% purity on a Quantachrome (NOVA 1200e) gas adsorption analyzer. Measurements were performed in the range of relative pressure from 0.05 to 0.99. Before the measurement, the sample was out gassed at 60 °C in the port of the sorption analyzer for three hours. Specific surface area was evaluated using the BET (Braunauer, Emmet and Teller) method and pore size distribution (PSD) was calculated using the BJH algorithm.

The electrical conductivity was measured by a four-point method using a Jandel Multi Height Probe with Jandel cylindrical probe head (25.4 nm diameter \times 48.5 nm high), tip spacing of 1.591 nm controlled by the RM3-AR Test Unit. The pressed pellets (15 mm in diameter and 0.50 mm in thickness, respectively) used in this measurement were prepared using 100 mg of the sample. Electrical conductivity of the pressed pellet was an average of eight values measured from two sides and in different places and it was determined for two different pellets.

3. Results and discussion

The choice for MCM-41 instead of other mesoporous silica was due to its easy preparation and its ordered one-dimensional parallel pores architecture at nanoscale range. The structural order and pores regularity of synthesized MCM-41 was proved respectively by the XRD and TEM (Fig. 1S and 2S – ESI†). The presence of diffraction peaks attributed to the (100) (110) and (200) planes are characteristic of a high ordered mesoporous silica.⁴⁶ The pore diameter and wall thickness estimated by TEM image are respectively 30 Å and 11 Å. The synthesized MCM-41 shows a hexagonal elongated shape and sharp size distribution of around 400 nm as observed in the SEM micrograph (Fig. 3S – ESI†).

The monomer adsorption in the MCM-41 pores was performed by vapor diffusion method to guarantee that aniline goes inside the pore and the polymer will be formed there posteriorly, as confirmed by N_2 adsorption isotherm experiments already published.⁶ The monomer adsorption process was monitored during 14 days, however since after the seventh day the mass kept constant, indicating the aniline saturation in the MCM-41 internal and external surfaces. In order to determine the amount of adsorbed aniline, the TGA curve was

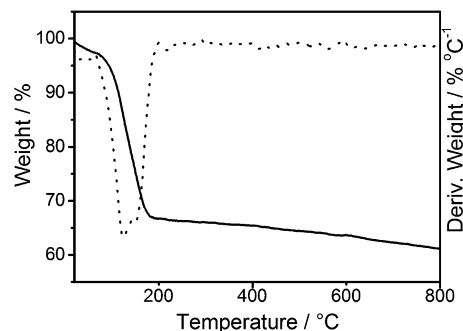
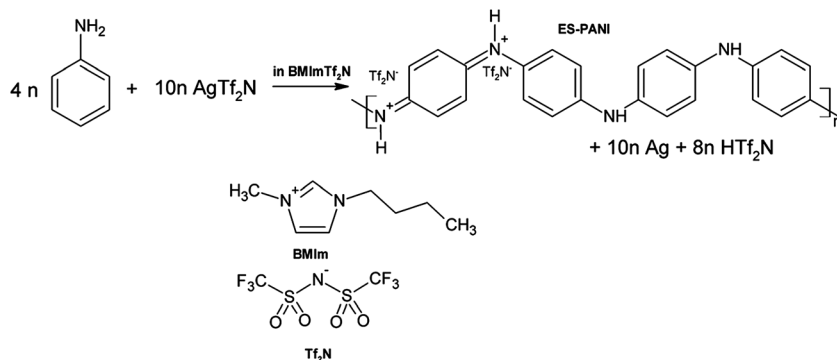


Fig. 2 TGA curve of MCM-41/Ani.



Scheme 1 Preparation of MCM-41/PANI/Ag composite in BMImTf₂N.

registered (Fig. 2) and the aniline loss was estimated to be around 33% (from room temperature until 200 °C). The presence of aniline was also confirmed by FTIR (Fig. 4S – ESI†).

After the aniline impregnation in the MCM-41 pores, the monomer was polymerized by AgTf₂N in BMImTf₂N, according to the chemical reaction described in Scheme 1, which was studied in our previous work.³⁵ This reaction is based on a simple oxidation of aniline by silver cations, which acts as oxidant agent and metal source. In ionic liquid, Ag⁺ was able to oxidize aniline to PANI quickly, which is not usual in aqueous media. One explanation for this fact is that the Ag⁺ reactivity dissolved in the ionic liquid is not equal to the reactivity observed in common organic solvents. In addition, considering that the oxidation of aniline to give the respective radical cation is the slow step³⁷ to obtain PANI, in our opinion the reaction occurs faster in ionic liquid than in aqueous medium, because the IL stabilizes this transition state more efficiently than water.

The isolated solid was green that is the characteristic color of PANI in its most conductive state, the emeraldine salt form (ES-PANI).

The X-ray diffraction pattern of MCM-41/PANI/Ag (Fig. 3) shows the characteristic low angle peaks of MCM-41 indicating that the *in situ* aniline polymerization did not cause the meso-structure collapse. With an enlargement of high angle region it is observed two diffraction peaks at 38° and 44° (inset in Fig. 3) that are attributed to (111) and (200) planes of the face-centered cubic phase of silver (ICDD file no. 4-0783). A bulky ES-PANI

sample shows two mainly broad diffraction peaks in the region of 20° to 25° attributed to the parallel arrangement periodicity of the polymeric chains.⁴⁸ These diffraction peaks were not observed in Fig. 3, suggesting that polymer chains were mostly generated inside the pores.

Analyzing the TGA curve of the MCM-41/PANI/Ag composite it is possible to observe one main event (Fig. 4) from 200 °C to 650 °C, which corresponds to 9% of weight loss and it was attributed to the polymer degradation. The onset temperature of the polymer decomposition is around 300 °C, indicating good thermal stability when compared to pure PANI. The residue (around 89%) corresponds to the silica and metallic silver.

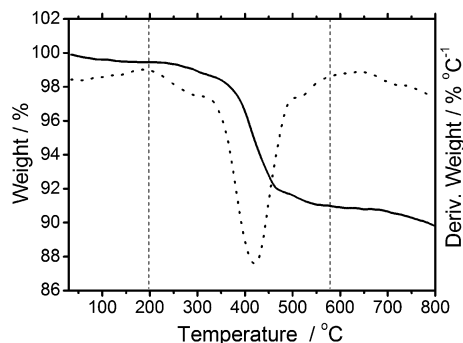


Fig. 4 TGA of the MCM-41/PANI/Ag composite.

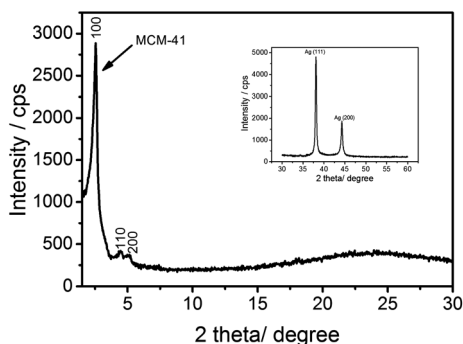


Fig. 3 X-ray diffraction pattern of the MCM-41/PANI/Ag composite.

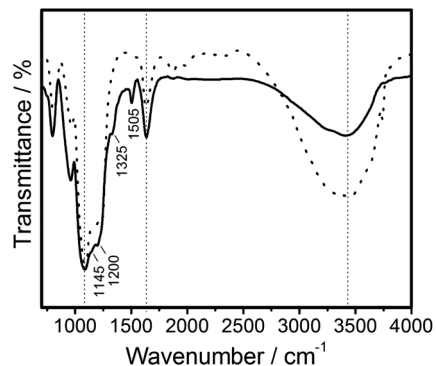


Fig. 5 FTIR spectra of the MCM-41/PANI/Ag composite (—) and pure MCM-41 (---).

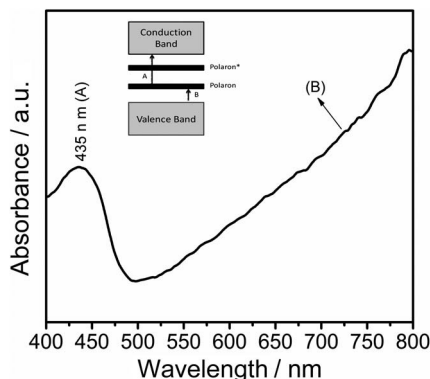


Fig. 6 UV-Vis electronic absorption spectrum of the MCM-41/PANI/Ag composite.

In order to prove the presence of PANI in the composite, the FTIR spectrum was registered (Fig. 5). The bands centered at 3425 cm^{-1} and 1630 cm^{-1} , observed also in the MCM-41 spectrum, are attributed to the O–H stretching and bending modes, respectively. The Si–O–Si stretching and bending vibrations occur at 1086 cm^{-1} and 800 cm^{-1} , respectively. The most notable differences comparing the MCM-41 and MCM-41/PANI/Ag spectra are the appearance of the band at 1505 cm^{-1} attributed to the benzenoid ring stretching vibration.^{49,50} The enlargement in the $1250\text{--}1100\text{ cm}^{-1}$ region comprises the band at 1145 cm^{-1} designated to the C–H in plane bending of the quinoid rings (oxidized units) of PANI. The presence of Tf_2N as counter ions of the positive charge of these oxidized units is confirmed by the appearance of the bands at 1200 cm^{-1} and 1325 cm^{-1} , which are designated to CF_3 and SO_2 stretching modes.⁵¹

In the UV-Vis spectrum (Fig. 6), registered in the solid state, it is observed two bands. The first centered at 435 nm is attributed to the polaron- π^* (A) transition and another that starts at 500 nm and extends until into the near infrared region assigned to π -polaron (B) transition, which is the most evidence of emeraldine salt formation.⁵² The surface plasmon resonance absorption of the electrons in the conducting silver bands usually observed around 400 nm can be overlapped by the absorption A of PANI.

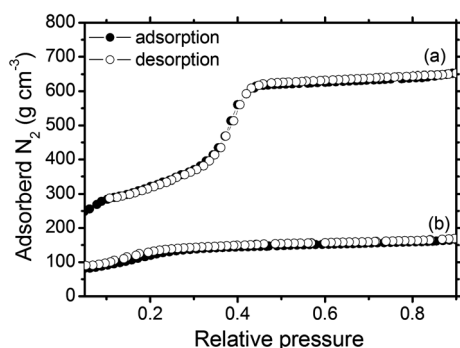


Fig. 7 N_2 adsorption-desorption isotherms of (a) MCM-41 and (b) MCM-41/PANI/Ag composite.

Table 1 Physical properties of MCM-41 and MCM-41/PANI/Ag samples

Sample	Surface area (BET) ($\text{m}^2\text{ g}^{-1}$)	Pore diameter (BJH) (\AA)	Pore volume (BHJ) ($\text{cm}^3\text{ g}^{-1}$)
MCM-41	1462	31.1	0.720
MCM-41/PANI/Ag	410	28.8	0.074

The N_2 adsorption-desorption isotherms for MCM-41 and MCM-41/PANI/Ag are shown in Fig. 7. MCM-41 shows a type IV-isotherm according to IUPAC classification.⁵³ The sharp increase in the adsorbed volume of N_2 at a relative pressure range of $P/P_0 = 0.3\text{--}0.4$ are due to capillary condensation of N_2 into mesopores.⁵⁴ The absence of hysteresis in the N_2 adsorption isotherms is a characteristic feature of small pore MCM-41.⁵⁵ Hysteresis is only observed in MCM-41 with pores larger than 40 \AA . There is not a confirmed explanation for this MCM-41 facet but it is suggested that it might be related to pore size heterogeneity.⁵⁶ Clearly in the MCM-41/PANI/Ag sample, the inflection point of the N_2 adsorption curve shifts to a lower value of relative pressure and above this point it is observed a long plateau that indicates less room to N_2 adsorb due to the presence of polymer and silver into the mesopores. The reduction of the surface area as well the pore volume for the composite corroborates the filling of the pores with PANI and silver, which partially blocks the adsorption of nitrogen molecules. Table 1 shows the physical parameter of nitrogen isotherms, such as BET surface area, pore volume and average pore diameter calculated from N_2 adsorption isotherms using the BJH model.

The morphology of the composite particles was analyzed by SEM (Fig. 8) and TEM (Fig. 9). It is not possible to identify segregated polymeric phases in the material or even silver particles. The aniline polymerization changed the silica particle size, since it is observed a considerable size decreasing when compared to the MCM-41 particle (Fig. 3S – ESI[†]). Small elongated cylindrical particles with diameters in the nanoscale range (around 100 nm) distributed homogeneously across the entire area of the substrate are observed after the polymerization, while before the silica particle size is estimated to be of the order of 400 nm.

The representative TEM images of the composite (Fig. 9) still exhibit elongated cylindrical particles (Fig. 9a) as observed in pure MCM-41. After the polymerization, the hexagonal structure, characteristic of the MCM-41, is noted in the composite (Fig. 9b and d), indicating that the present preparation method had no effect on the uniform structure of the MCM-41. The presence of silver was confirmed by energy dispersive X-ray spectroscopy (EDX) (Fig. 9c). Only a very small amount of silver nanoparticles (diameter around 5 nm), indicated by the arrows, are observed outside the pore channels.

Finally, the electrical conductivity of the composite, evaluated using a four probe method, was in the order of 10^{-3} S cm^{-1} , which is one million higher than the conductivity of MCM-41/PANI composite (*ca.* 10^{-9} S cm^{-1}),¹⁴ since silicas are an electrical isolating material in general. Considering that to achieve good electrical conductivity, the polymeric chains of

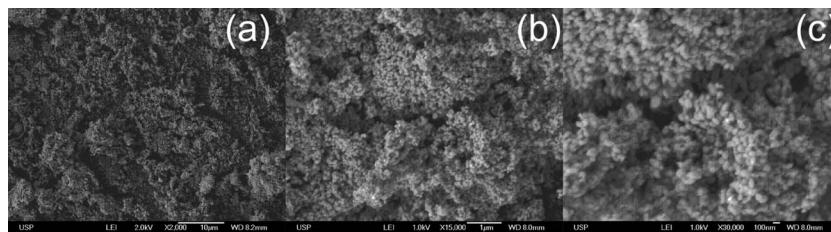


Fig. 8 SEM images of the MCM-41/PANI/Ag composite.

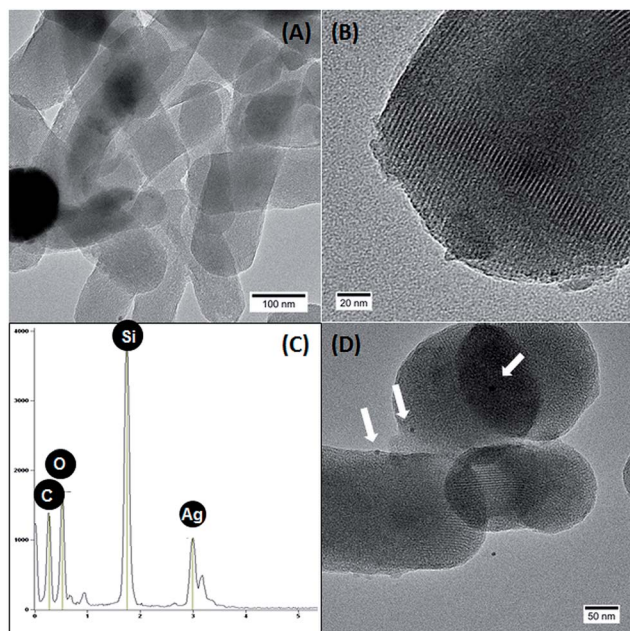


Fig. 9 TEM images of the MCM-41/PANI/Ag composite registered at different magnifications (a, b and d) and EDX spectrum of the composite (c).

polyaniline should have contact to each other in order to promote the intrachain and interparticle charge transports, it is evident that in the dual composite (silica and polyaniline) this chain connectivity is not occurring effectively. Therefore, our proposal is that the Ag nanoparticles produced inside the pores improve the charge transport among the polyaniline particles produced inside the pores, enhancing the electrical conductivity of the whole material. By comparing the conductivity values of bulk PANI and silver with the composite, it can be seen that this value is lower for the latter, indicating that most of the composite is located inside the channels than on the outer surface of the MCM-41.

4. Conclusions

In this work, it was shown a one-pot synthetic procedure of a ternary nanocomposite based on mesoporous silica with pores filled with polyaniline and metallic silver nanoparticles. In ionic liquid, silver cations are able to oxidize the aniline monomer in a fast rate reaction, producing at the same time polyaniline and silver nanoparticles. The size of the Ag particles and the direction of polymeric chain growth are constraint by the MCM-41

pores size and shape. The presence of silver nanoparticles in the MCM-41/PANI composite increased the electrical conductivity at about 10^6 times.

Acknowledgements

The authors acknowledge the Brazilian agency FAPESP (Grant Number 07/50742-2) for financial support and are thankful to Prof. Vera R. L. Constantino (IQ-USP) for the X-ray diffraction and UV-Vis experiments, to microscopy support of C2NANO – Center for Nanoscience and Nanotechnology/MCT (TEM-MS-C-15017 proposal) and to Laboratório de Simulação e Controle de Processos (POLI-USP) for the TGA analysis.

References

- 1 P. Gomez-Romero, *Adv. Mater.*, 2001, **13**, 163.
- 2 L. Nicole, L. Rozes and C. Sanchez, *Adv. Mater.*, 2010, **22**, 3208.
- 3 C. Sanchez, B. Julia, P. Belleville and M. Popall, *J. Mater. Chem.*, 2005, **15**, 3559.
- 4 D. Zhang and Y. Wang, *Mater. Sci. Eng., B*, 2006, **134**, 9.
- 5 H. D. Tran, D. Li and R. B. Kaner, *Adv. Mater.*, 2009, **21**, 1487.
- 6 C. G. Wu and T. Bein, *Science*, 1994, **264**, 1757.
- 7 M. S. Cho, H. J. Choi, K. Y. Kim and W. S. Ahn, *Macromol. Rapid Commun.*, 2002, **23**, 713.
- 8 Q. Cheng, V. Pavlinek, A. Lengalova, C. Li, Y. He and P. Saha, *Microporous Mesoporous Mater.*, 2006, **93**, 263.
- 9 R. Guo, G. Li, W. Zhang, G. Shen and D. Shen, *ChemPhysChem*, 2005, **6**, 2025.
- 10 O. A. Anunziata, M. B. G. Costa and R. D. Sánchez, *J. Colloid Interface Sci.*, 2005, **292**, 509.
- 11 X. M. Feng, G. Yang, Y. G. Liu, W. H. Hou and J. J. Zhu, *J. Appl. Polym. Sci.*, 2006, **101**, 2088.
- 12 E. Flores-Loyla, R. Cruz-Silva, J. Romero-Garcia, J. L. Ângulo-Sanchez, F. F. Castillon and M. H. Farias, *Mater. Chem. Phys.*, 2007, **105**, 136.
- 13 C. M. S. Izumi, V. R. L. Constantino and M. L. A. Temperini, *J. Phys. Chem. B*, 2005, **109**, 22131.
- 14 M. S. Cho, H. J. Choi and W. S. Ahn, *Langmuir*, 2004, **20**, 202.
- 15 H. J. Choi, M. S. Cho and W. S. Ahn, *Synth. Met.*, 2003, **135**, 711.
- 16 S. Ameen, Y.-B. Im, C. G. Jo, Y. S. Kim and H.-S. Shin, *J. Nanosci. Nanotechnol.*, 2011, **11**, 541.
- 17 L. C. Fonseca, R. Faez, F. F. Camilo and M. A. Bizeto, *Microporous Mesoporous Mater.*, 2012, **159**, 24.

- 18 R. A. Barros, C. R. Martins and W. M. Azevedo, *Synth. Met.*, 2005, **155**, 35.
- 19 D. Y. Shin and I. Kim, *Nanotechnology*, 2009, **20**, 415301.
- 20 A. Kitani, T. Akashi, K. Sugimoto and S. Ito, *Synth. Met.*, 2001, **121**, 1301.
- 21 A. Drelinkiewicz, M. Hasik and M. Kloc, *Catal. Lett.*, 2000, **64**, 41.
- 22 P. T. Radford and S. E. Creager, *Anal. Chim. Acta*, 2001, **449**, 199.
- 23 Y. Gao, D. Shan, F. Cao, J. Gong, X. Li, H. Y. Ma, Z. M. Su and K. Y. Qu, *J. Phys. Chem. C*, 2009, **113**, 15175.
- 24 S. K. Pillalamarri, F. D. Blum, A. T. Tokuhira and M. F. Bertino, *Chem. Mater.*, 2005, **17**, 5941.
- 25 J. Du, Z. Liu, B. Han, Z. Li, J. Zhang and Y. Huang, *Microporous Mesoporous Mater.*, 2005, **84**, 254.
- 26 J. Li, H. Tang, A. Zhang, X. Shen and L. Zhu, *Macromol. Rapid Commun.*, 2007, **28**, 740.
- 27 R. A. Barros and W. M. Azevedo, *Synth. Met.*, 2008, **158**, 922.
- 28 N. V. Blinova, J. Stejskal, M. Trchova, I. Sapurina and G. Ciric-Marjanovic, *Polymer*, 2009, **50**, 50.
- 29 K. Gupta, P. C. Jana and A. K. Meikap, *Synth. Met.*, 2010, **160**, 1566.
- 30 W. M. Azevedo, R. A. Barros and E. F. Silva Jr, *J. Mater. Sci.*, 2012, **43**, 400.
- 31 N. V. Blinova, P. Bober, J. Hromadkova, M. Trchova, J. Stejskal and J. Prokes, *Polym. Int.*, 2010, **59**, 437.
- 32 S. Bouazza, V. Alonzo and D. Hauchard, *Synth. Met.*, 2009, **159**, 1612.
- 33 A. B. Afzal, M. J. Akhtar, M. Nadeem, M. M. Ahmad, M. M. Hassan, T. Yasin and M. Mehmood, *J. Phys. D: Appl. Phys.*, 2009, **42**, 015411.
- 34 J. Stejskal, M. Trchova, J. Kovarova, L. Brozova and J. Prokes, *React. Funct. Polym.*, 2009, **69**, 86.
- 35 C. M. Correa, R. Faez, M. Bizeto and F. F. Camilo, *RSC Adv.*, 2012, **2**, 3088.
- 36 J. Dupont, *J. Braz. Chem. Soc.*, 2004, **15**, 341.
- 37 L. Leclercq and A. Schmitzer, *Supramol. Chem.*, 2009, **21**, 245.
- 38 Y. Zhou, J. H. Schattka and M. Antonietti, *Nano Lett.*, 2004, **4**, 477.
- 39 L. L. Lazarus, C. T. Riche, N. Malmstadt and R. L. Brutchey, *Langmuir*, 2012, **28**, 15987.
- 40 D. Pahovnik, E. Zagar, J. Vohlidal and M. Zigon, *Synth. Met.*, 2010, **160**, 1761.
- 41 H.-J. Kim, S.-H. Park and H.-J. Park, *Radiat. Phys. Chem.*, 2010, **79**, 894.
- 42 H.-J. Kim, S.-H. Park and H.-J. Park, *Sens. Lett.*, 2011, **9**, 59.
- 43 K. M. Manesh, A. I. Gopalan, K. P. Lee and S. Komathi, *Catal. Commun.*, 2010, **11**, 913.
- 44 P. Bonhote, A. P. Dias, N. Papageorgiou, K. Kalyanasundaram and M. Graetzel, *Inorg. Chem.*, 1996, **35**, 1168.
- 45 Q. Cai, W. Y. Lin, F. S. Xiao, W. Q. Pang, X. H. Chen and B. S. Zou, *Microporous Mesoporous Mater.*, 1999, **32**, 1.
- 46 C. Y. Chen, S. Q. Xiao and M. E. Davis, *Microporous Mater.*, 1995, **4**, 1.
- 47 N. C. Billingham, S. P. Armes, M. T. Gill, S. E. Chapman, C. L. Dearmitt, F. L. Baines, C. M. Dadswell, J. G. Stamper and G. A. Lawless, *Synth. Met.*, 1998, **93**, 227.
- 48 L. Zhang and M. Wan, *Adv. Funct. Mater.*, 2003, **13**, 815.
- 49 Y. Furukawa, F. Ueda, Y. Hyodo, I. Harada, T. Nakajima and T. Kawagoe, *Macromolecules*, 1998, **21**, 1297.
- 50 M. Trchova and J. Stejskal, *Pure Appl. Chem.*, 2011, **83**, 1803.
- 51 M. J. Muldoon and C. M. Gordon, *J. Polym. Sci., Part A: Polym. Chem.*, 2004, **42**, 3865.
- 52 J. Stejskal, P. Kratochvil and N. Radhakrishnan, *Synth. Met.*, 1993, **61**, 225.
- 53 K. S. W. Sing, D. H. Everett, R. A. W. Haul, L. Moscou, R. A. Pierotti, J. Rouquerol and T. Siemieniowska, *Pure Appl. Chem.*, 1985, **57**, 603.
- 54 P. J. Branton, P. G. Hall and K. S. W. Sing, *J. Chem. Soc., Chem. Commun.*, 1993, 1257.
- 55 M. Kruk, M. Jaroniec and A. Saiary, *J. Phys. Chem. B*, 1997, **101**, 583.
- 56 M. W. Maddox and K. E. Gubbins, *Int. J. Thermophys.*, 1994, **15**, 1115.